

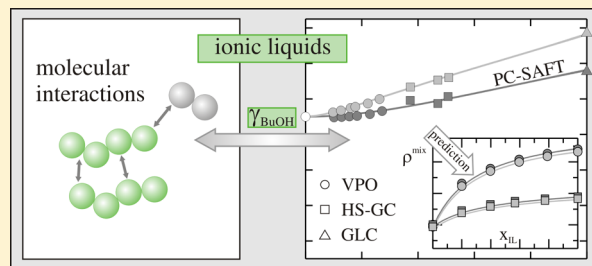
Molecular Interactions in 1-Butanol + IL Solutions by Measuring and Modeling Activity Coefficients

Alexander Nann,[†] Jan Mündges,[†] Christoph Held,[†] Sergey P. Verevkin,[‡] and Gabriele Sadowski^{*,†}

[†]Laboratory of Thermodynamics, Department of Biochemical and Chemical Engineering, Technische Universität Dortmund, Emil-Figge-Str. 70, 44227 Dortmund, Germany

[‡]Department of Physical Chemistry, University of Rostock, Dr. Lorenz-Weg 1, 18059 Rostock, Germany

ABSTRACT: Molecular interactions in 1-butanol + ionic liquid (IL) solutions have been investigated by measuring and modeling activity-coefficient data. The activity coefficients in binary solutions containing 1-butanol and an IL were determined experimentally: the ILs studied were 1-decyl-3-methyl-imidazolium tetracyanoborate ($[\text{Im}_{10.1}]^+[\text{tcb}]^-$), 4-decyl-4-methyl-morpholinium tetracyanoborate ($[\text{Mo}_{10.1}]^+[\text{tcb}]^-$), 1-decyl-3-methyl-imidazolium bis-(trifluoromethylsulfonyl)imide ($[\text{Im}_{10.1}]^+[\text{ntf}_2]^-$), and 4-decyl-4-methyl-morpholinium bis-(trifluoromethylsulfonyl)imide ($[\text{Mo}_{10.1}]^+[\text{ntf}_2]^-$). The methods used to determine the activity coefficients included vapor-pressure osmometry, headspace-gas chromatography, and gas-liquid chromatography. The results from all of these techniques were combined to obtain activity-coefficient data over the entire IL concentration range, and the ion-specific interactions of the ILs investigated were identified with 1-butanol. The highest (1-butanol)–IL interactions of the ILs considered in this work were found for $[\text{Im}_{10.1}]^+[\text{tcb}]^-$; thus, $[\text{Im}_{10.1}]^+[\text{tcb}]^-$ showed the highest affinity for 1-butanol in a binary mixture. The experimental data were modeled with the Perturbed-Chain Statistical Associating Fluid Theory (PC-SAFT). PC-SAFT was able to accurately describe the pure IL and (1-butanol)–IL data. Moreover, the model was shown to be predictive and extrapolative with respect to concentration and temperature.



INTRODUCTION

Ionic liquids (ILs) are organic salts that usually consist of a large organic cation and a small inorganic anion. Due to the asymmetry of the anion and cation, many ILs are known to be stable as liquids over a broad temperature range.¹ The enormous variety of possible anion–cation combinations allows for the development and design of task-specific ILs (“tailor-made solvents”).² A large number of ILs have interesting and unique properties, in particular a negligible vapor pressure at ambient temperatures and a high thermal and chemical stability,³ that have aroused considerable interest in application to novel technologies and applied science, e.g., in biotechnology,⁴ biocatalysis,⁵ and electrochemistry,⁶ as well as in chemical engineering and separation processes.^{1,7} ILs are also considered to be new agents for the liquid–liquid extraction^{8–10} of a variety of organic and inorganic compounds.

In the past decade, ionic liquids have been extensively investigated with respect to their structure, physical and thermodynamic properties, as well as their feasible applications.^{7,11} However, the accurate characterization and modeling of the thermodynamic properties of ILs and IL solutions still remains an active research subject. Thus, more systematic studies on IL solutions are highly desirable regarding physical and thermodynamic properties, modeling strategies, and molecular interaction behavior.

In previous studies, two methods have been found to be suitable for the determination of vapor–liquid equilibria

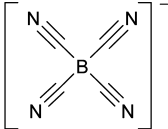
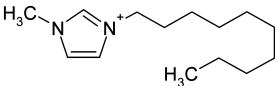
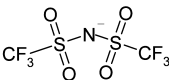
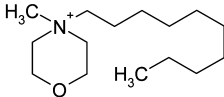
(VLEs) in IL solutions: vapor-pressure osmometry (VPO) and headspace-gas chromatography (HS-GC).^{12–23} The main advantages of VPO are the small sample amounts required, the low experimental time needed, and the high accuracy of the procedure.²⁴ Calvar et al. and Gomez et al.^{12–17} investigated imidazolium- and pyridinium-based ILs with the anions methylsulfate, ethylsulfate, and bis(trifluoromethylsulfonyl)imide in binary solutions containing several alcohols and water, using VPO measurements up to an IL molality of 3 mol/kg (mole of IL/kg of pure solvent) at a temperature of 323.15 K.

The HS-GC method has also been shown to be successful for measuring the vapor-pressure data of binary and ternary solutions containing ILs. Sadr and Sardroodi²³ determined the osmotic coefficients of binary mixtures of acetone and bis(tetraalkylammonium)-tetrathiomolybdates (three different bis(tetraalkylammonium)-tetrathiomolybdates were studied) up to a salt molality of 1 mol/kg at 298.15 K. Kim et al.²⁵ investigated the isothermal vapor pressures of ternary solutions containing an IL (where 1-ethyl-3-methylimidazolium ethylsulfate and 1-butyl-3-methylimidazolium tetrafluoroborate were the ILs studied), at a temperature of 333.15 K up to an IL mole fraction of 0.2. Most studies of solutions containing ILs have

Received: July 23, 2012

Revised: February 3, 2013

Table 1. Anions and Cations of the Following Ionic Liquids in This Study: $[\text{Im}_{10.1}]^+[\text{tcb}]^-$, $[\text{Mo}_{10.1}]^+[\text{tcb}]^-$, $[\text{Im}_{10.1}]^+[\text{ntf}_2]^-$, and $[\text{Mo}_{10.1}]^+[\text{ntf}_2]^-$

anions	cations
 <p>tetracyanoborate $[\text{tcb}]^-$</p>	 <p>1-decyl-3-methyl-imidazolium $[\text{Im}_{10.1}]^+$</p>
 <p>bis(trifluoromethylsulfonyl)imide $[\text{ntf}_2]^-$</p>	 <p>4-decyl-4-methyl-morpholinium $[\text{Mo}_{10.1}]^+$</p>

focused on aqueous systems. For example, Shekaari et al.^{18–21} investigated binary solutions of water or acetonitrile with several ILs. Gardas et al.²² have studied aqueous solutions containing 1-ethyl-3-methylimidazolium bromide or 1-butyl-3-methylimidazolium chloride. One shortcoming of the published VPO and HS-GC data is that the IL concentrations have been low (the highest concentration was only 3 mol/kg). Gas-liquid chromatography (GLC) has also been found to be a reliable complementary method for measuring solute activity coefficients at infinite dilution in an IL.^{26,27}

The molecular complexity of ILs, the presence of dispersive, electrostatic, and associative interactions,²⁸ as well as the tendency of ILs to form ion pairs²⁹ and aggregates³⁰ are challenging for any modeling approach. The growing base of experimental data can be used to analyze, correlate, and model the thermo-physical data and phase behavior of pure ILs and IL solutions. Often, g^E models, such as the extended Pitzer model or the modified NRTL model, have been used to describe the experimental data.^{12–23} In addition to these two correlations, other approaches (such as COSMO-RS and SAFT) have also been applied to model the thermodynamic properties of IL systems. Further information can be found in Vega et al.,³¹ which gives a comprehensive review of various modeling approaches.

Recently, Padaszyński and Domańska³² used PC-SAFT^{33,34} (Perturbed-Chain Statistical Associating Fluid Theory) to model pure-IL data and the binary liquid–liquid equilibria of mixtures composed of piperidinium and bis(trifluoromethylsulfonyl)imide-based ILs with alcohols, hydrocarbons, and water. The pure-IL parameters were determined by fits to pure-IL densities and IL-solubility data that were determined from Hildebrand parameters at different temperatures and ambient pressures. The temperature-dependent binary interaction parameters were adjusted to activity coefficients at infinite dilution in the ILs. Other authors have also successfully applied PC-SAFT to model IL solutions.^{35–37}

The experimental component of this work focused on determining the pure-IL and IL-solution densities, vapor–liquid equilibria (VLE), and activity coefficients at infinite dilution for various binary mixtures containing ILs. The ionic liquids 1-decyl-3-methyl-imidazolium tetracyanoborate ($[\text{Im}_{10.1}]^+[\text{tcb}]^-$),

4-decyl-4-methyl-morpholinium tetracyanoborate ($[\text{Mo}_{10.1}]^+[\text{tcb}]^-$), 1-decyl-3-methyl-imidazolium bis(trifluoromethylsulfonyl)imide ($[\text{Im}_{10.1}]^+[\text{ntf}_2]^-$), and 4-decyl-4-methyl-morpholinium bis(trifluoromethylsulfonyl)imide ($[\text{Mo}_{10.1}]^+[\text{ntf}_2]^-$) were investigated in their pure states and in binary solutions with 1-butanol. These ILs have technical importance as promising extracting agents in separation processes. New experimental density and activity-coefficient data for the systems considered are reported in this study. The experimental techniques of VPO, HS-GC, and GLC were used to determine the 1-butanol activity coefficients. The results of the different experimental methods were combined to obtain activity-coefficient data over the entire IL concentration range. The experimental results were analyzed in terms of the association behavior between the ions as well as the molecular (1-butanol)–IL interactions as a function of the composition and type of anion–cation combination. The PC-SAFT equation of state was used to model the data. The pure-component IL parameters were evaluated using the pure-IL density data, the VPO data, and the 1-butanol activity coefficients at infinite dilution. The pure-component IL parameters were then used to calculate and predict a variety of thermodynamic properties such as the 1-butanol partial pressures and the (1-butanol)–IL solution densities.

EXPERIMENTAL WORK

Materials. 1-Butanol was purchased from VWR International GmbH at a purity higher than 99.8 wt % and was used without further purification. The purity of the liquid was confirmed by GLC before use. The four ionic liquids, $[\text{Im}_{10.1}]^+[\text{tcb}]^-$, $[\text{Mo}_{10.1}]^+[\text{tcb}]^-$, $[\text{Im}_{10.1}]^+[\text{ntf}_2]^-$, and $[\text{Mo}_{10.1}]^+[\text{ntf}_2]^-$, that were studied in this work were obtained from Merck KGaA. Table 1 illustrates the different ions present in these ILs.

All of the ionic liquids were dried by vacuum evaporation at 338 K for over 12 h to remove traces of any volatile chemicals and water. The mass fraction of water was determined by Karl Fischer titration using a Mettler-Toledo DL31 titrator. The water concentration was found to be less than 0.07 wt %. All of the samples were stored under a nitrogen atmosphere. The vapor-pressure osmometer was calibrated using LiBr (>99 wt

%) from Sigma-Aldrich Chemie GmbH without further purification. The GLC column packing consisted of Chromosorb PAW-DMDCS 100/120 mesh as the solid support, which was coated with an IL. All of the IL solution samples were prepared directly before performing the experiments. The solution components were weighed using a Satorius CC 1201 precision balance with a resolution of $\pm 10^{-4}$ g.

Density Measurements. The densities of the pure ILs and the 1-butanol + IL solutions were measured using a vibrating-tube densimeter “DMA 602” from Anton Paar GmbH, Germany. The maximum uncertainty specified by the manufacturer was lower than $\pm 1.5 \times 10^{-6}$ g/cm³. The densimeter was calibrated at atmospheric pressure with air and deionized water.³⁸ The densities of the pure ILs were determined at atmospheric pressure at temperatures ranging from 293.15 to 363.15 K; the IL solution densities were measured at atmospheric pressure and temperatures ranging from 303.15 to 333.15 K for IL mole fractions between 0.2 and 0.8.

Vapor-Pressure Osmometry. Measurements were performed using a KNAUER vapor-pressure osmometer K-7000. The measuring cell consisted of a glass beaker that was filled with the solvent (1-butanol in this work) and saturated with 1-butanol vapor. Two thermistors were immersed into the cell. The measuring cell was placed in a thermostat. The cell temperature was electronically controlled to an accuracy of $\pm 1 \times 10^{-3}$ K. Prior to performing an experiment, the apparatus signal was adjusted to zero by placing pure 1-butanol droplets on each thermistor. This was accomplished by using microsyringes in all the experiments. Stable signals were reached after 5 min. Afterward, one 1-butanol droplet was replaced by a droplet of IL solution (1-butanol + IL). The addition of an IL reduced the chemical potential of the 1-butanol in the solution droplet. The difference between the chemical potentials of 1-butanol in the IL-solution droplet and the pure 1-butanol droplet caused 1-butanol vapor to condense onto the IL-solution droplet. Due to the condensation, the solution-droplet temperature increased. The change in temperature (ΔT) caused a change in resistance (ΔR), which was detected via a Wheatstone bridge connected to both thermistors.

Care was taken in placing droplets of reproducible sizes and shapes onto both thermistors, as has been recommended elsewhere.²⁴ For each sample, at least three ΔR values were reported and the mean value was calculated. The measurements were carried out for binary 1-butanol + IL solutions at 323.15 K and IL concentrations up to 5 mol/kg (corresponding to IL mole fractions up to 0.32). Within this concentration range, the maximum standard deviation of the measured values was approximately 3%.

The osmotic coefficient ϕ was obtained as a function of molality m_i from the measured resistance difference ΔR via

$$\phi = \frac{\Delta R \cdot K}{\nu \cdot m_i} \quad (1)$$

where K is the calibration constant and ν is the stoichiometric number of the solute. This number was considered to be equal to unity in this work (assuming the solute did not dissociate into ions and did not agglomerate). Prior to performing an experiment, the calibration constant K was determined by measuring the ΔR values for LiBr solutions of known molalities. Plotting $\Delta R/\nu \cdot m$ versus $\nu \cdot m$ yielded the reciprocal of the calibration constant from extrapolating to zero molality,

as suggested by Solie.²⁴ This procedure was proofed by comparing measured osmotic coefficients for ethanol–LiBr systems with literature data.³⁹ The measurements were carried out at 323.15 K and atmospheric pressure for LiBr concentrations ranging between 50 and 100 mmol/kg. An osmotic coefficient of 0.746 at 70 mmol/kg was found for this concentration range. The deviation between the experimental osmotic coefficient and the literature value³⁹ (0.723 at 70 mmol/kg) was estimated to be within 2.2%.

Headspace-Gas Chromatography. Headspace-gas chromatography (HS-GC) was used to determine the partial pressures, activities, and activity coefficients of 1-butanol in binary 1-butanol + IL solutions at 323.15 K for IL mole fractions ranging from 0.37 to 0.51. The 1-butanol vapor phase in equilibrium with the (1-butanol)–IL solution was analyzed by this method. The HS-GC measurements were carried out using an Agilent 7890A gas chromatograph equipped with an autosampler, a thermal conductivity detector, and a HP-INNOWax capillary column. A thermostat for 21 sample vials (10 mL) was heated with a 70 W heat-cartridge and was located on top of the gas chromatograph. The vials were maintained at 323.15 ± 0.5 K. The equilibration time of the sample vials was investigated between 8 and 16 h. As the 1-butanol peak areas for the two samples (one sample was equilibrated for 8 h, and the other sample was equilibrated for 16 h) were equal within the experimental uncertainty (2–4%, see below), the phases were assumed to be equilibrated after 8 h. Prior to performing the headspace measurements, the sample vials were tempered for 8 h. After that, 0.7 mL of the gas volume was injected into the gas chromatograph.

The main advantage of the headspace technique is that only volatile components are injected into the column. Due to negligible vapor pressure, the ILs do not need to be considered in the vapor composition analysis. The only volatile component in the 1-butanol + IL systems considered was 1-butanol; the activity of 1-butanol (denoted by the index 1 in this work) in the sample can be directly calculated using the following relation:

$$a_1 = \frac{p_{1,IL}}{p_{01}^{LV}} = \frac{A_{1,IL}^{\text{exp}}}{A_{01}} \quad (2)$$

where $A_{1,IL}^{\text{exp}}$ denotes the detected peak area of 1-butanol in the 1-butanol + IL sample at temperature T and A_{01} denotes the detected peak area of 1-butanol in the pure 1-butanol sample at the same temperature. All measurements were repeated three times. Over the investigated concentration range up to 0.51 IL mole fraction, the maximum standard deviation for the peak area was found to be in the 2–4% range, depending on the IL being studied.

Gas-Liquid Chromatography. Gas-liquid chromatography measurements were used to determine the 1-butanol activity coefficients at infinite dilution in ILs at different temperatures. The experimental procedure has been described in detail elsewhere.²⁶ The experiments were carried out using a Hewlett-Packard 5890 Series II gas chromatograph equipped with a flame ionization detector. Nitrogen was used as the carrier gas and was purified via an Agilent RMSN-2 gas purification cartridge prior to use. A packed column made of a stainless-steel tube, with a length of approximately 40 cm and an inside diameter of 0.4 cm, was used.

The column was filled with a known amount (<3 g) of the solid support, Chromosorb PAW-DMDCS 100/120 mesh,

which was coated with the respective IL to form the stationary phase. The coating process was carried out in a round-bottomed flask, by weighing defined masses of the solid support and the IL that were then dispersed in dichloromethane. Afterward, the dichloromethane was evaporated moderately using a rotational evaporator. The solid support and the IL were weighed with a Satorius CPA 324S precision balance with an accuracy of $\pm 2 \times 10^{-4}$ g. To avoid residual adsorption activity of the support material, the quantity of the IL stationary phase was adjusted to approximately 30% relative to the weight of the solid support, as has been recommended elsewhere.²⁶ Prior to performing the experiments, the column was maintained at 353.15 K and flushed with nitrogen overnight to remove residual volatile impurities and water. Thus, the GLC apparatus was free of volatiles prior to the measurements.

The pressure drop ($p^{\text{in}} - p^{\text{out}}$) inside the column was varied between 50 and 100 kPa depending on retention times and peak shapes. The inlet pressure p^{in} of the column was measured to an accuracy of ± 0.1 kPa using a Keller Leo 2 digital manometer mounted on the gas chromatograph. The outlet pressure p^{out} of the column was assumed to be equal to atmospheric pressure,²⁶ which was determined by a GE Druck DPI 740 precision pressure barometer with a precision of ± 0.02 kPa. The flow rate of the carrier gas was measured at the outlet of the gas chromatograph using an Agilent ADM 1000 gas-flow meter with an accuracy of ± 0.2 mL·min⁻¹. The flow rates were measured systematically after each change of the inlet pressure p^{in} or the column temperature. The experiments were performed at five temperatures ranging from 323.15 to 363.15 K. The temperature of the GC column was maintained constant to within ± 0.05 K.

Pure samples, with a volume ranging from 0.2 to 0.4 μL depending on the peak shapes, were injected. No deviations in the retention times t_r were observed as a function of the injected volumes. Thus, 1-butanol was assumed to be at infinite dilution in the IL column. At a given temperature, each measurement was performed at least three times, and the mean retention time was calculated. The retention times were generally reproducible within ± 0.03 min. The absolute values of the retention times were adjusted to be between 4 and 40 min, depending on the temperature and flow rate, in order to obtain sharp peaks and well-defined retention times. The column stability was checked every 8 h by measuring the 1-butanol retention time at 343.15 K.

Methane was assumed to be the nonretainable component²⁶ in order to measure the dead time t_G at each temperature. The dead time values are required for calculating the 1-butanol activity coefficients at infinite dilution.

The following equation, which was developed by Everett⁴⁰ and Cruickshank,⁴¹ was used to determine the 1-butanol activity coefficients at infinite dilution $\gamma_{1,\text{IL}}^\infty$ in an IL.

$$\ln \gamma_{1,\text{IL}}^\infty = \ln \left(\frac{n_{\text{IL}} RT}{V_{\text{N}} p_{01}^{\text{LV}}} \right) - \frac{(B_{11} - v_{01}) p_{01}^{\text{LV}}}{RT} + \frac{(2B_{12} - v_1^\infty) J p^{\text{out}}}{RT} \quad (3)$$

In eq 3, n_{IL} is the mole number of the IL (stationary phase) immobilized on the column packing, T is the column temperature, p_{01}^{LV} is the vapor pressure of 1-butanol at temperature T , B_{11} is the second virial coefficient of pure 1-butanol, B_{12} is the cross virial coefficient of 1-butanol and the

carrier gas nitrogen (index 2), v_{01} is the liquid molar volume of 1-butanol at temperature T , v_1^∞ is the partial molar volume of 1-butanol in the IL at infinite dilution at temperature T , R is the universal gas constant, and p^{out} is the pressure at the column outlet.

The net retention volume V_{N} of 1-butanol was obtained using the following equation:⁴²

$$V_{\text{N}} = J U_0 (t_{\text{R}} - t_{\text{G}}) \quad (4)$$

where U_0 is the flow rate at the column outlet. t_{R} and t_{G} are the retention times for 1-butanol and the nonretainable component (methane), respectively. The factor J in eqs 3 and 4 is related to the pressure drop along the column as follows:⁴²

$$J = \frac{3(p^{\text{in}}/p^{\text{out}})^2 - 1}{2(p^{\text{in}}/p^{\text{out}})^3 - 1} \quad (5)$$

The values for the virial coefficients, B_{11} and B_{12} , were calculated using equations that have been developed by Tsionopoulos.⁴³ The critical quantities (p^c , T^c , and V^c) and the acentric factor Z that were used to calculate the virial coefficients were obtained using values and equations from the literature.⁴⁴ The temperature-dependent p_{01}^{LV} values were determined using the Antoine equation with Antoine constants from the literature.⁴⁵ The molar volume v_{01} of 1-butanol was determined using the experimental 1-butanol densities measured in this work. The partial molar volume of 1-butanol at infinite dilution v_1^∞ in an IL was assumed to be equal to v_{01} , as has been proposed elsewhere.²⁶ Taking into account the uncertainties in the column loading, retention time, and flow rate, the activity coefficients at infinite dilution were estimated to be accurate within $\pm 5\%$. Reproducibility measurements showed deviations of less than $\pm 5\%$ in the activity coefficients at infinite dilution for measurements using different columns containing the same IL.

■ THERMODYNAMIC MODELING

PC-SAFT. The PC-SAFT equation of state is composed of a reference term that represents repulsion between molecules and is perturbed by additive attractive-energy contributions to account for van der Waals attractions and association. PC-SAFT is particularly appropriate for IL systems compared to other SAFT-based models because the nonspherical shape of the molecules is explicitly accounted for in the reference term.

PC-SAFT calculates the residual Helmholtz energy a^{res} of a system as a sum of several independent contributions:

$$a^{\text{res}} = a^{\text{hc}} + a^{\text{disp}} + a^{\text{assoc}} + a^{\text{polar}} \quad (6)$$

In eq 6, a^{hc} is the Helmholtz energy of the reference hard-chain fluid, while a^{disp} and a^{assoc} denote the dispersive and associative Helmholtz-energy contributions. A detailed description of the contributions has been given by Gross and Sadowski.^{33,34} The Helmholtz-energy contribution from polar interactions is accounted for by a^{polar} . Although ILs are assumed to have non-negligible dipole moments,³⁷ previous studies have shown that the polar term only has a slight influence.³⁷ Thus, the polar term was neglected in this work.

In PC-SAFT, a nonassociating component i is characterized by the following three pure-component parameters: the segment number m_i^{seg} , the segment diameter σ_i , and the dispersion-energy parameter u_i/k_{B} . The associative contribution requires two additional parameters: the association-energy parameter $\epsilon^{A,B_i}/k_{\text{B}}$ and the association-volume parameter κ^{A,B_i} .

Table 2. Experimental Liquid Densities of Pure ILs ρ_{IL} in a Temperature Range between 293.15 and 343.15 K at Atmospheric Pressure

T (K)	ρ_{IL} ($\text{kg}\cdot\text{m}^{-3}$)			
	$[\text{Im}_{10.1}]^+[\text{tcb}]^-$	$[\text{Mo}_{10.1}]^+[\text{tcb}]^-$	$[\text{Im}_{10.1}]^+[\text{ntf}_2]^-$	$[\text{Mo}_{10.1}]^+[\text{ntf}_2]^-$
293.15	967.69	985.87	1282.54	1288.79
303.15	960.72	979.30	1273.62	1280.67
313.15	953.75	972.65	1264.73	1272.27
323.15	947.14	966.30	1256.24	1264.37
333.15	940.48	960.01	1247.51	1256.35
343.15	933.44	953.45	1238.16	1247.91

Two identical association sites were assumed for each IL, as well as for 1-butanol (2B model).

The mixture parameters for modeling binary solutions are usually estimated using the conventional Lorentz–Berthelot combining rules:

$$\sigma_{ij} = \frac{1}{2}(\sigma_i + \sigma_j) \quad (7)$$

$$u_{ij} = \sqrt{u_i u_j} (1 - k_{ij}) \quad (8)$$

where k_{ij} is the binary interaction parameter that corrects for the deviation of the dispersion-energy parameter between unlike molecules from that obtained using the geometric mean of the pure-component parameters. In this work, all k_{ij} values were set to zero. As the ILs in this work were considered to form ion pairs, dispersion among the IL molecules was taken into account. However, the charge–charge interactions among the ILs were neglected.

The strength of the cross-association interactions between two associating substances can be described by the combining rules suggested by Wolbach and Sandler:⁴⁶

$$\varepsilon^{A_i B_j} = \frac{1}{2}(\varepsilon^{A_i B_i} + \varepsilon^{A_j B_j}) \quad (9)$$

$$\kappa^{A_i B_j} = \sqrt{\kappa^{A_i B_i} \kappa^{A_j B_j}} \left(\frac{\sqrt{\sigma_i \sigma_j}}{\frac{1}{2}(\sigma_i + \sigma_j)} \right)^3 \quad (10)$$

Calculation of Activity Coefficients with PC-SAFT. The activity coefficient γ_i of a component i is defined as the ratio of the fugacity coefficient of the component i φ_i^{L} , at a concentration x_i in a mixture, and the fugacity coefficient of the pure liquid component φ_{0i}^{L} :

$$\gamma_i = \frac{\varphi_i^{\text{L}}(T, p, x_i)}{\varphi_{0i}^{\text{L}}(T, p, x_i = 1)} \quad (11)$$

The fugacity coefficients can be calculated with PC-SAFT. The exact relationship is given elsewhere.⁴⁷

The activity coefficient at infinite dilution is calculated using the following equation:

$$\gamma_i^\infty = \frac{\varphi_i^{\infty, \text{L}}(T, p, x_i \rightarrow 0)}{\varphi_{0i}^{\text{L}}(T, p, x_i = 1)} \quad (12)$$

where $\varphi_{0i}^{\infty, \text{L}}$ is the fugacity coefficient at infinite dilution. This value can be determined using PC-SAFT as well.

RESULTS AND DISCUSSION

Experimental Densities of Pure ILs and IL Solutions.

The experimental densities of pure ILs ρ_{IL} were measured over

a temperature range between 293.15 and 343.15 K; the densities of the binary 1-butanol + IL solutions ρ_{mix} were determined at atmospheric pressure for temperatures ranging from 303.15 to 333.15 K and for IL mole fractions between 0.2 and 0.8. The results are summarized in Tables 2 and 3 and shown in Figures 1 and 2.

Table 3. Experimental Liquid-Density Data ρ_{mix} of Binary Solutions (1-Butanol + IL) as a Function of IL Mole Fraction and Temperature at Atmospheric Pressure

x_{IL}	ρ_{mix} [$\text{kg}\cdot\text{m}^{-3}$]			
	303.15 K	313.15 K	323.15 K	333.15 K
	$[\text{Im}_{10.1}]^+[\text{tcb}]^-$			
0.201	880.44	873.13	866.07	858.78
0.392	914.80	907.33	899.76	891.72
0.595	927.55	921.79	917.22	916.05
0.789	950.17	943.21	936.43	929.81
	$[\text{Mo}_{10.1}]^+[\text{tcb}]^-$			
0.199	890.94	883.60	876.37	868.52
0.398	930.49	923.20	916.58	910.54
0.567	950.66	943.86	937.36	930.75
0.773	967.12	960.56	954.09	947.60
	$[\text{Im}_{10.1}]^+[\text{ntf}_2]^-$			
0.199	1048.88	1040.16	1031.23	1022.02
0.398	1152.00	1142.08	1131.72	1120.49
0.598	1209.55	1200.92	1192.35	1183.77
0.803	1248.23	1239.67	1231.18	1222.68
	$[\text{Mo}_{10.1}]^+[\text{ntf}_2]^-$			
0.200	1063.58	1055.09	1045.97	1036.00
0.397	1157.98	1149.65	1141.51	1133.12
0.595	1215.98	1207.70	1199.32	1192.03
0.790	1252.83	1244.06	1235.00	1223.80

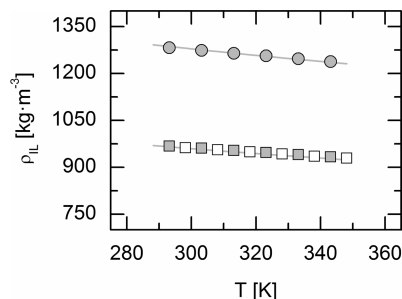


Figure 1. Experimental liquid-density data of pure ionic liquids ρ_{IL} as a function of temperature at atmospheric pressure; symbols represent experimental data points: $[\text{Im}_{10.1}]^+[\text{ntf}_2]^-$ (circles); $[\text{Im}_{10.1}]^+[\text{tcb}]^-$ (filled squares); ref 48 (open squares); and solid lines (—) are calculations using the PC-SAFT model.

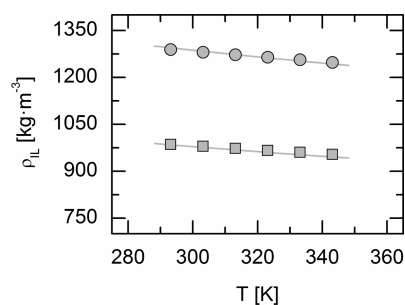


Figure 2. Experimental liquid-density data of pure ionic liquids ρ_{IL} as a function of temperature at atmospheric pressure; symbols represent experimental data points: $[\text{Mo}_{10,1}]^+[\text{ntf}_2]^-$ (circles); $[\text{Mo}_{10,1}]^+[\text{tcb}]^-$ (squares); and solid lines (—) are calculations using the PC-SAFT model.

The density values for pure $[\text{Im}_{10,1}]^+[\text{tcb}]^-$ are in good accordance with literature data published by Domańska and Marciniak,⁴⁸ as shown in Figure 1. The experimental densities were correlated using a linear fit with a maximum deviation of less than 0.02% to allow for a comparison with literature data. The maximum deviation of the literature data⁴⁸ from this correlation was 0.2%. The density of a liquid is known to depend on the size and shape of the molecules (steric effects), the molecular weight, and molecular interactions. In general, high substance densities are obtained for high molar masses, strong attractive interactions, and compact molecular structures. The densities of the pure ILs investigated in this work strongly increase with increasing molar mass and decrease with increasing temperature. A comparison of the pure-IL densities revealed a density dependence on the anion–cation combination of the ILs under consideration. On the one hand, ILs with identical anions and different cations possess very similar pure-liquid densities: the densities of the $[\text{Mo}_{10,1}]^+$ -containing ILs are only slightly higher than the densities of the $[\text{Im}_{10,1}]^+$ -based ILs. In contrast, anions have a much stronger influence on IL densities: replacing the $[\text{tcb}]^-$ anion by $[\text{ntf}_2]^-$ has a very pronounced influence on the IL density. The modeling results that are shown in Figures 1 and 2 will be discussed later in the modeling section.

The concentration dependence of the solution densities is illustrated in Figures 3 and 4. The densities increase more strongly for solutions containing ILs of higher molar mass. As expected from the pure-IL experimental data, the densities of

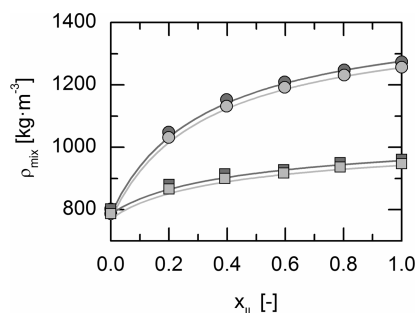


Figure 3. Experimental liquid density ρ_{mix} of (1-butanol + IL) solutions as a function of the IL mole fraction for ILs containing the $[\text{Im}_{10,1}]^+$ cation at $T = 323.15$ K (light gray) and $T = 303.15$ K (dark gray) and atmospheric pressure; symbols represent experimental data points: $[\text{Im}_{10,1}]^+[\text{ntf}_2]^-$ (circles); $[\text{Im}_{10,1}]^+[\text{tcb}]^-$ (squares); and solid lines (—) are the PC-SAFT model predictions.

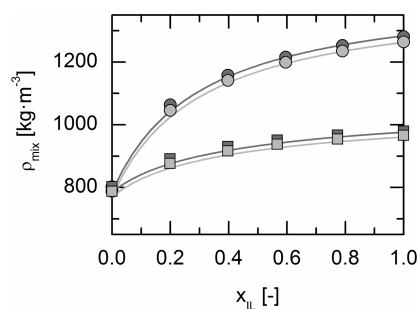


Figure 4. Experimental liquid density ρ_{mix} of (1-butanol + IL) solutions as a function of the IL mole fraction for ILs containing the $[\text{Mo}_{10,1}]^+$ cation at $T = 323.15$ K (light gray) and $T = 303.15$ K (dark gray) and atmospheric pressure; symbols represent experimental data points: $[\text{Mo}_{10,1}]^+[\text{ntf}_2]^-$ (circles); $[\text{Mo}_{10,1}]^+[\text{tcb}]^-$ (squares); and solid lines (—) are the PC-SAFT model predictions.

ILs containing the $[\text{Im}_{10,1}]^+$ cation are slightly lower than those of the $[\text{Mo}_{10,1}]^+$ -containing ILs. The solution densities of the $[\text{ntf}_2]^-$ -based ILs are considerably higher than those of the $[\text{tcb}]^-$ -containing ILs. Moreover, an increase in the mixture density with decreasing temperature is observed. Both dependencies are as expected and are well-known from the density behavior of many other compounds.

Experimental Data of Partial Pressures and Activity Coefficients. The experimental osmotic coefficients of the binary solutions of 1-butanol + IL studied here were measured using the VPO method over IL mole fractions ranging from 0.07 to 0.32 at $T = 323.15$ K.

Using the original definition for the osmotic coefficients,⁴⁹ the osmotic coefficients were converted into activity coefficients and activities by using the following equations:

$$\gamma_1 = e^{(\phi-1)\ln x_1} \quad (13)$$

$$a_1 = \gamma_1 x_1 \quad (14)$$

where γ_1 is the 1-butanol activity coefficient, ϕ is the osmotic coefficient, x_1 is the 1-butanol mole fraction, and a_1 is the 1-butanol activity.

The partial pressures of 1-butanol p_1 in solutions with IL were calculated using the following equation

$$\ln(a_1) = \ln\left(\frac{p_1}{p_{01}^{\text{LV}}}\right) + \frac{(B_{11} + v_{01})(p_1 - p_{01}^{\text{LV}})}{RT} \quad (15)$$

which had to be solved iteratively with respect to p_1 . The values and constants required in the calculations were determined using the methods described in the GLC section.

Table 4 summarizes the resulting activities, activity coefficients, and partial pressures of 1-butanol in the binary systems with ILs from the VPO measurements. The uncertainties for the activity coefficients and partial pressures were calculated by Gaussian error propagation using the average deviations determined for the ΔR values of the VPO measurements. The maximum uncertainties were estimated to be within $\pm 1\%$ for the activity coefficients as well as for the partial pressures. Especially considering the comparatively high IL concentrations up to 0.32 IL mole fraction, this is a very good result.

The 1-butanol activities in the binary solutions of 1-butanol + IL, for IL concentrations ranging from 0.37 to 0.51 IL mole fraction at 323.15 K, were measured via HS-GC. The 1-butanol

Table 4. Experimental Activities a_1 , Activity Coefficients γ_1 , and Partial Pressures p_1 of 1-Butanol Determined via VPO in Binary (1-Butanol + IL) Solutions as a Function of the IL Mole Fraction at 323.15 K

x_{IL}	a_1	γ_1	p_1 (kPa)
$[\text{Im}_{10.1}]^+[\text{tcb}]^-$			
0.069	0.917	0.985	4.239
0.099	0.898	0.997	4.152
0.129	0.860	0.987	3.974
0.157	0.837	0.992	3.867
0.182	0.825	1.009	3.813
0.229	0.796	1.033	3.680
0.266	0.775	1.056	3.582
$[\text{Mo}_{10.1}]^+[\text{tcb}]^-$			
0.100	0.927	0.995	4.285
0.139	0.897	0.998	4.147
0.170	0.877	1.006	4.052
0.201	0.858	1.016	3.966
0.230	0.839	1.027	3.878
0.278	0.817	1.059	3.775
0.322	0.804	1.105	3.718
$[\text{Im}_{10.1}]^+[\text{ntf}_2]^-$			
0.069	0.951	1.021	4.394
0.101	0.931	1.036	4.304
0.130	0.916	1.052	4.232
0.165	0.894	1.071	4.131
0.183	0.890	1.088	4.112
0.228	0.862	1.117	3.985
0.270	0.851	1.166	3.932
$[\text{Mo}_{10.1}]^+[\text{ntf}_2]^-$			
0.067	0.961	1.029	4.441
0.098	0.948	1.051	4.383
0.126	0.939	1.074	4.342
0.160	0.929	1.106	4.293
0.177	0.922	1.120	4.261
0.222	0.907	1.165	4.191
0.263	0.899	1.220	4.157

activities in the binary system of 1-butanol + $[\text{Im}_{10.1}]^+[\text{ntf}_2]^-$ were determined over a broader concentration range of 0.13–0.51 IL mole fraction, yielding additional experimental results to those obtained for the concentration range of the VPO method (0.07–0.32). The experimentally determined 1-butanol activities were converted into 1-butanol activity coefficients and partial pressures by using eqs 14 and 15. Table 5 reports the resulting activities, activity coefficients, and partial pressures of 1-butanol in the 1-butanol + IL binary systems at $T = 323.15$ K from the HS-GC measurements. As the VPO method was used for IL mole fractions between 0.07 and 0.32, the results from the two independent methods were used as proof of conformity between the VPO and HS-GC data.

The dependence of the 1-butanol partial pressures on the IL mole fraction at 323.15 K is shown in Figures 5 and 6 for all the 1-butanol + IL solutions under consideration. These figures show that the HS-GC data is in good agreement with the apparent trend for the partial pressures that were determined via VPO. The maximum relative deviation between the experimental 1-butanol partial pressures determined using VPO and HS-GC, respectively, is less than 2.1%.

The 1-butanol partial pressures are directly linked to the molecular interactions in the system. In general, the lower the 1-butanol partial pressures, the higher are the (1-butanol)–IL

Table 5. Experimental Activities a_1 , Activity Coefficients γ_1 , and Partial Pressures p_1 of 1-Butanol Determined via HS-GC in Binary (1-Butanol + IL) Solutions as a Function of the IL Mole Fraction at 323.15 K

x_{IL}	a_1	γ_1	p_1 (kPa)
$[\text{Im}_{10.1}]^+[\text{tcb}]^-$			
0.373	0.706	1.126	3.263
0.470	0.565	1.065	2.608
0.509	0.534	1.088	2.467
$[\text{Mo}_{10.1}]^+[\text{tcb}]^-$			
0.372	0.743	1.184	3.436
0.470	0.609	1.149	2.814
0.507	0.606	1.227	2.798
$[\text{Im}_{10.1}]^+[\text{ntf}_2]^-$			
0.129	0.926	1.063	4.281
0.206	0.872	1.098	4.030
0.271	0.816	1.119	3.771
0.372	0.790	1.257	3.652
0.472	0.704	1.333	3.255
0.570	0.571	1.326	2.637
$[\text{Mo}_{10.1}]^+[\text{ntf}_2]^-$			
0.373	0.837	1.333	3.867
0.470	0.748	1.412	3.458
0.509	0.706	1.439	3.264

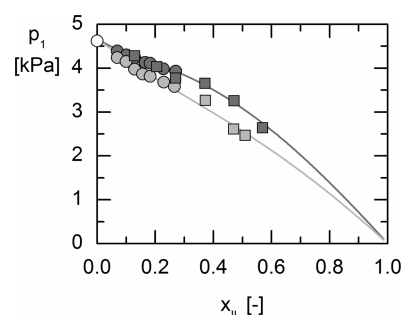


Figure 5. Experimental partial pressures p_1 of 1-butanol in binary (1-butanol + IL) solutions as a function of the IL mole fraction for ILs containing the $[\text{Im}_{10.1}]^+$ cation: $[\text{Im}_{10.1}]^+[\text{ntf}_2]^-$ (dark gray) and $[\text{Im}_{10.1}]^+[\text{tcb}]^-$ (light gray) at 323.15 K; symbols represent experimental data points: VPO (circles); HS-GC (squares); and solid lines (—) are calculations using the PC-SAFT model.

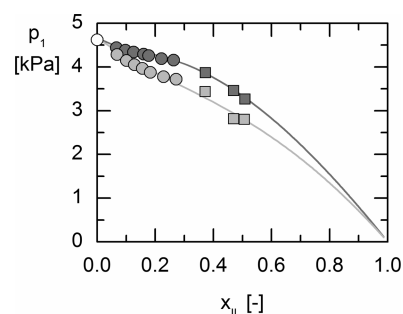


Figure 6. Experimental partial pressures p_1 of 1-butanol in (1-butanol + IL) solutions as a function of the IL mole fraction for ILs containing the cation $[\text{Mo}_{10.1}]^+$ ($[\text{Mo}_{10.1}]^+[\text{ntf}_2]^-$ (dark gray) and $[\text{Mo}_{10.1}]^+[\text{tcb}]^-$ (light gray)) at 323.15 K; symbols represent experimental data points: VPO (circles); HS-GC (squares); and solid lines (—) are calculations using the PC-SAFT model.

interactions. Thus, the 1-butanol partial pressure is high in systems with low (1-butanol)–IL interactions.

Depending on the anion–cation combination of the ILs studied, the IL influence on the 1-butanol partial pressures is more or less pronounced. The 1-butanol partial pressures in binary 1-butanol + IL solutions for ILs with identical anions are very similar; that is, replacing $[\text{Im}_{10.1}]^+$ with $[\text{Mo}_{10.1}]^+$ has a rather small influence on the (1-butanol)–IL interactions. This behavior can be ascribed to the similar chemical structure of the cations (see Table 1). Both cations are comparable in size and charge distribution. Only the chemical composition of the ring structure differs for these cations. Obviously, this difference in the chemical structure produces a difference in the (1-butanol)–IL interactions for the ILs containing these cations. Slightly lower 1-butanol partial pressures are observed for solutions containing ILs with the $[\text{Im}_{10.1}]^+$ cation. Thus, it can be concluded that ILs with the $[\text{Im}_{10.1}]^+$ cation cause stronger (1-butanol)–IL interactions compared to ILs with the $[\text{Mo}_{10.1}]^+$ cation.

The influence of the IL anions is higher than that of the IL cations. As illustrated in Figures 5 and 6, the $[\text{tcb}]^-$ anion causes considerably lower 1-butanol partial pressures than $[\text{ntf}_2]^-$. This behavior is ion-specific, occurring independently of the type of cation and the IL concentration. The anions have distinctly different molecular sizes, shapes, and charge distributions.

Summarizing the effects of the cations and anions, it can be concluded that the higher the 1-butanol partial pressure, the lower is the (1-butanol)–IL interaction, in accordance with the following trend: $[\text{Im}_{10.1}]^+[\text{tcb}]^- > [\text{Mo}_{10.1}]^+[\text{tcb}]^- > [\text{Im}_{10.1}]^+[\text{ntf}_2]^- > [\text{Mo}_{10.1}]^+[\text{ntf}_2]^-$. These results indicate that $[\text{Im}_{10.1}]^+[\text{tcb}]^-$ has the highest affinity for 1-butanol in a binary mixture compared to the other ILs investigated.

The IL activity coefficients were used to analyze the IL–IL interactions in 1-butanol + IL systems. The osmotic-coefficient data can be converted into IL activity coefficients using the Gibbs–Duhem relation.⁴⁷ For this purpose, the experimental osmotic coefficients were approximated by a power series as follows:

$$\phi - 1 = \sum_{r=1}^q \alpha_r m_{\text{IL}}^r \quad (16)$$

where the α_r values are constants of the power series with the index r , m_{IL}^r is the IL molality raised to the power of the respective index, and q refers to the number of parameters needed to represent the experimental osmotic coefficients. This series was converted into the IL activity coefficients γ_{IL}^* (with the standard state being the hypothetical ideal solution) using

$$\ln \gamma_{\text{IL}}^* = (\phi - 1) + \int_0^{m_{\text{IL}}} \frac{(\phi - 1)}{m_{\text{IL}}} dm_{\text{IL}} \quad (17)$$

The lower the IL activity coefficients, the stronger are the IL–IL interactions. Figure 7 shows that the activity coefficients of all ILs are always below unity; that is, the ILs in the binary 1-butanol + IL solution interact strongly with each other, and the solvation effects ((1-butanol)–IL interactions) are less pronounced. The $[\text{ntf}_2]^-$ anion produces considerably lower IL activity coefficients than $[\text{tcb}]^-$. The influence of the cations is less pronounced; that is, replacing $[\text{Im}_{10.1}]^+$ by $[\text{Mo}_{10.1}]^+$ has only a weak influence on the IL activity coefficients. The lowest IL activity coefficients for the 1-butanol + IL solutions under consideration are found for $[\text{Mo}_{10.1}]^+[\text{ntf}_2]^-$, whereas the highest IL–IL interactions are observed for $[\text{Mo}_{10.1}]^+[\text{ntf}_2]^-$. The following trend for the IL–IL interactions in solution with

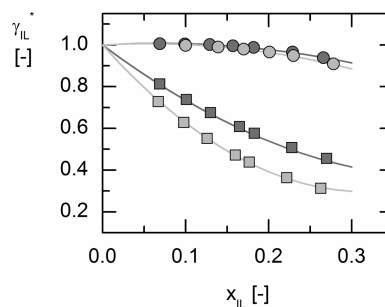


Figure 7. Experimental IL activity coefficients in binary 1-butanol + IL solutions as a function of the IL mole fraction at 323.15 K; symbols represent experimental data: $[\text{tcb}]^-$ -based ILs (circles) (dark gray, $[\text{Im}_{10.1}]^+[\text{tcb}]^-$; light gray, $[\text{Mo}_{10.1}]^+[\text{tcb}]^-$) and $[\text{ntf}_2]^-$ -based ILs (squares) (dark gray, $[\text{Im}_{10.1}]^+[\text{ntf}_2]^-$; light gray, $[\text{Mo}_{10.1}]^+[\text{ntf}_2]^-$); and solid lines (—) drawn to guide the eye.

1-butanol was observed for the series of ILs studied: $[\text{Mo}_{10.1}]^+[\text{ntf}_2]^- > [\text{Im}_{10.1}]^+[\text{ntf}_2]^- > [\text{Mo}_{10.1}]^+[\text{tcb}]^- > [\text{Im}_{10.1}]^+[\text{tcb}]^-$. Comparing the trends for the (1-butanol)–IL interactions and the IL–IL interactions, it can be concluded that the higher the (1-butanol)–IL interactions, the lower are the IL–IL interactions in the binary systems under consideration.

Finally, the activity coefficients of 1-butanol at infinite dilution in the ILs under consideration were determined via the GLC method for temperatures ranging from 323.15 to 363.15 K. As previously described, the activity coefficients at infinite dilution were estimated to be accurate within $\pm 5\%$. The γ_1^∞ values for 1-butanol in the four ILs are summarized in Table 6.

Table 6. Experimental Activity Coefficients at Infinite Dilution γ_1^∞ of 1-Butanol in the Ionic Liquids under Consideration for Temperatures Ranging from 323.15 to 363.15 K

	T (K)				
	323.15	333.15	343.15	353.15	363.15
$[\text{Im}_{10.1}]^+[\text{tcb}]^-$	1.42	1.34	1.29	1.25	1.22
$[\text{Mo}_{10.1}]^+[\text{tcb}]^-$	1.51	1.44	1.37	1.33	1.29
$[\text{Im}_{10.1}]^+[\text{ntf}_2]^-$	1.64	1.54	1.47	1.40	1.36
$[\text{Mo}_{10.1}]^+[\text{ntf}_2]^-$	1.94	1.82	1.70	1.64	1.57

The 1-butanol activity coefficients at infinite dilution in this study were slightly higher than the experimental values published by Domańska and Marciniak⁴⁸ for 1-butanol in $[\text{Im}_{10.1}]^+[\text{tcb}]^-$ at temperatures between 323.15 and 363.15 K. These differences in the activity coefficients at infinite dilution may result from the data-reduction step. In the work of Domańska and Marciniak, a correction term for the partial pressure of water was used in the net retention volume calculations. In this work, this correction term was discarded as the GLC apparatus was free of water, as has been described in the GLC section. Furthermore, the literature⁵⁰ shows that deviations of up to 20% in the activity coefficients at infinite dilution, as measured by GLC, between different laboratories are typical. The deviations between the experimental values in this work and the literature data are $<15\%$, so that the 1-butanol activity coefficients at infinite dilution are within a reasonable range.

Figure 8 shows the logarithm of the activity coefficient at infinite dilution versus the reciprocal temperature.

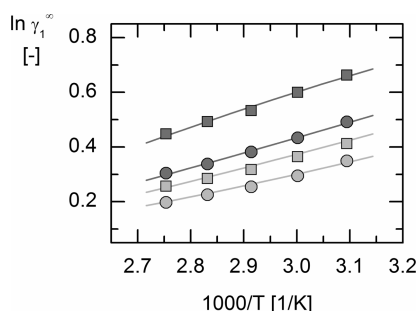


Figure 8. Experimental values of $\ln \gamma_1^\infty$ as a function of $1000/T$ for 1-butanol in ILs containing the following anions: $[tcb]^-$ ($[Im_{10.1}]^+[tcb]^-$ (light gray circles) and $[Mo_{10.1}]^+[tcb]^-$ (light gray squares)); $[ntf_2]^-$ ($[Im_{10.1}]^+[ntf_2]^-$ (dark gray circles) and $[Mo_{10.1}]^+[ntf_2]^-$ (dark gray squares)); and solid lines (—) are calculations using the PC-SAFT model.

For all ILs (independent of the respective cations and anions), the 1-butanol activity coefficients at infinite dilution increase with decreasing temperature over the temperature range investigated. Comparing the results for all the ILs studied, the 1-butanol activity coefficients at infinite dilution are lowest for ILs containing $[Im_{10.1}]^+[tcb]^-$. Thus, the highest (1-butanol)–IL interactions are found for ILs containing $[Im_{10.1}]^+[tcb]^-$, again yielding the following trend: $[Im_{10.1}]^+[tcb]^- > [Mo_{10.1}]^+[tcb]^- > [Im_{10.1}]^+[ntf_2]^- > [Mo_{10.1}]^+[ntf_2]^-$. Thus, the conclusions from the VPO and HS-GC data are confirmed.

The limiting partial molar excess enthalpies $\bar{h}_1^{E,\infty}$ and entropies $\bar{s}_1^{E,\infty}$ of 1-butanol were obtained from the experimental activity coefficients at infinite dilution by using the following equation:

$$\ln \gamma_1^\infty = \frac{\bar{h}_1^{E,\infty}}{RT} - \frac{\bar{s}_1^{E,\infty}}{R} \quad (18)$$

Assuming a linear temperature dependence for the logarithm of the activity coefficients at infinite dilution, the limiting partial molar excess enthalpy $\bar{h}_1^{E,\infty}$ was determined from the slope of the linear fit of $\ln \gamma_1^\infty$ vs $1000/T$. The linear correlations are accurate within an average deviation of less than $\pm 2\%$. The uncertainties of the calculated limiting partial molar excess enthalpies $\bar{h}_1^{E,\infty}$ and entropies $\bar{s}_1^{E,\infty}$ were estimated to within $\pm 1\%$. The limiting partial molar excess entropy $\bar{s}_1^{E,\infty}$ was obtained from the y-axis intercept. All the calculated $\bar{h}_1^{E,\infty}$ and $\bar{s}_1^{E,\infty}$ values for 1-butanol are listed in Table 7.

Table 7. Limiting Partial Molar Excess Enthalpies $\bar{h}_1^{E,\infty}$ and Entropies $\bar{s}_1^{E,\infty}$ of 1-Butanol in the ILs Investigated

	$\bar{h}_1^{E,\infty}$ (kJ·mol ⁻¹)	$\bar{s}_1^{E,\infty}$ (J·mol ⁻¹ ·K ⁻¹)
$[Im_{10.1}]^+[tcb]^-$	3.7	8.5
$[Mo_{10.1}]^+[tcb]^-$	3.8	8.4
$[Im_{10.1}]^+[ntf_2]^-$	4.6	10.2
$[Mo_{10.1}]^+[ntf_2]^-$	5.2	10.8

All the $\bar{h}_1^{E,\infty}$ values obtained for 1-butanol are positive for the systems studied. The lower the $\bar{h}_1^{E,\infty}$ value of 1-butanol in the respective IL, the more advantageous is the mixing of the components and the stronger the (1-butanol)–IL interactions in the solutions. Lower $\bar{h}_1^{E,\infty}$ values resulted from the $[tcb]^-$ -based ILs than the $[ntf_2]^-$ -based ILs. Thus, ILs containing $[tcb]^-$ exert considerably stronger (1-butanol)–IL interactions

than ILs containing the $[ntf_2]^-$ anion. The lowest positive $\bar{h}_1^{E,\infty}$ value of 1-butanol is found in solutions with $[Im_{10.1}]^+[tcb]^-$, again showing that the highest molecular interactions between 1-butanol and an IL are found in the 1-butanol + $[Im_{10.1}]^+[tcb]^-$ solution for the systems investigated in this work.

The (1-butanol)–IL interactions decrease in the order $[Im_{10.1}]^+[tcb]^- > [Mo_{10.1}]^+[tcb]^- > [Im_{10.1}]^+[ntf_2]^- > [Mo_{10.1}]^+[ntf_2]^-$. Thus, the molecular-interaction behavior analyzed using the $\bar{h}_1^{E,\infty}$ values yields the same trend that was observed in the (1-butanol)–IL interactions by analyzing the 1-butanol partial pressures. The $\bar{s}_1^{E,\infty}$ values for 1-butanol are small and positive for all the ILs under consideration.

The activity-coefficient data over the entire IL concentration range could be analyzed by combining the data measured by VPO and HS-GC with the infinite dilution activity coefficients. The results are shown in Figures 9 and 10 for all the IL solutions considered.

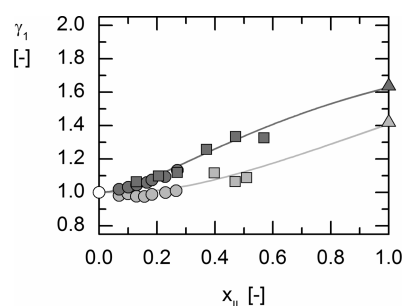


Figure 9. Experimental activity coefficients γ_1 of 1-butanol as a function of the IL mole fraction in binary solutions (1-butanol + IL) at 323.15 K for ILs containing the following cations: $[Im_{10.1}]^+$ ($[Im_{10.1}]^+[tcb]^-$ (light gray) and $[Im_{10.1}]^+[ntf_2]^-$ (dark gray)); symbols represent experimental data points: VPO (circles), HS-GC (squares), GLC (triangles); and solid lines (—) are calculations using the PC-SAFT model.

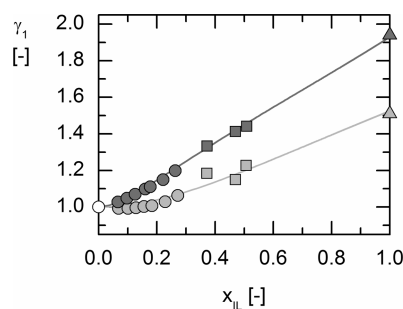


Figure 10. Experimental activity coefficients γ_1 of 1-butanol as a function of the IL mole fraction in binary solutions (1-butanol + IL) at 323.15 K for ILs containing the following cations: $[Mo_{10.1}]^+$ ($[Mo_{10.1}]^+[tcb]^-$ (light gray) and $[Mo_{10.1}]^+[ntf_2]^-$ (dark gray)); symbols represent experimental data: VPO (circles), HS-GC (squares), GLC (triangles); and solid lines (—) are calculations using the PC-SAFT model.

Figures 9 and 10 show that the 1-butanol activity coefficients determined via the VPO, HS-GC, and GLC methods mesh together very well. Thus, the activity-coefficient data was obtained over the entire range of IL concentrations. Starting from a value of unity, the 1-butanol activity coefficients increase with increasing IL concentrations. Among the ILs considered, the lowest and highest activity coefficients over the entire range

were found for solutions containing $[\text{Im}_{10.1}]^+[\text{tcb}]^-$ and $[\text{Mo}_{10.1}]^+[\text{ntf}_2]^-$, respectively.

The Gibbs–Duhem equation requires that the 1-butanol activity coefficients and the IL activity coefficients in a 1-butanol + IL solution are related to each other. In particular, increasing 1-butanol activity coefficients lead to decreasing IL activity coefficients.⁴⁷ A concentration-dependent association behavior is well-known for inorganic electrolytes in organic solvents, as well as in water.⁵¹ The results of a study by Nasirzadeh et al.⁵² on the association behavior of electrolytes in organic solvents lead to the conclusion that the higher the 1-butanol activity coefficients, the higher the tendency of the IL ions to form ion associates. For the 1-butanol activity coefficients in the systems considered here, this association behavior is strongly distinctive for $[\text{ntf}_2]^+$ -based ILs at small IL concentrations compared to $[\text{tcb}]^-$ -based ILs, which appear to be at least partially dissociated under dilute conditions. Thus, the IL ions considered strongly tend to form ion associates in concentrated 1-butanol + IL solutions. These results confirm the assumption of IL-ion pairs that was used in the data reduction and modeling. This assumption could also be confirmed by analyzing the IL activity coefficients. In the solutions considered, all the IL activity coefficients were found to be below unity and the series of their quantitative values was found to be in accordance with the results described above; that is, the ILs tend to form ion pairs in the sequence $[\text{Im}_{10.1}]^+[\text{tcb}]^- < [\text{Mo}_{10.1}]^+[\text{tcb}]^- < [\text{Im}_{10.1}]^+[\text{ntf}_2]^- < [\text{Mo}_{10.1}]^+[\text{ntf}_2]^-$.

Modeling Results. Some assumptions were made to model the systems under consideration by PC-SAFT. The ILs were considered to be nondissociated and nonaggregated. This assumption is reasonable based on the actual experience regarding the ion-pairing behavior of ionic liquids in concentrated solutions²⁹ and the association phenomena discussed above.

Therefore, the ILs studied were treated as molecules with distinctive association behavior, as has been previously considered in the literature.^{32,37,53} However, in contrast to previous studies, the 2B approach was used throughout this work, which assumes that one association site represents the positive group of the IL and one site represents the negative group of the IL. The IL molecules are allowed to interact with each other and with 1-butanol via hard-chain repulsion, dispersion, and association. Multipolar forces were not considered in this work.

The five pure-component PC-SAFT parameters for the ILs, namely, the segment number, the segment diameter, the dispersion-energy parameter, and the two association parameters, were determined from fits to the experimental temperature-dependent liquid densities of the pure ILs, the binary VPO data at 323.15 K, and the 1-butanol activity coefficients at infinite dilution for the respective IL over the temperature range investigated. Thus, the mixture densities and the HS-GC data were not included in the parameter estimation. The PC-SAFT parameters for 1-butanol were taken from the literature.³⁴ All the model parameters used in this work are summarized in Table 8.

The deviation between the modeled (mod) and the experimental data (exp) for a quantity z was evaluated in terms of average relative deviations (ARD) that were calculated using the following equation:

Table 8. PC-SAFT Model Parameters for the ILs Investigated and 1-Butanol^a

	σ_i (Å)	m_i^{seg}	u_i/k_B (K)	$\varepsilon^{A,B_i}/k_B$ (K)	κ^{A,B_i}
$[\text{Im}_{10.1}]^+[\text{tcb}]^-$	4.1876	7.598	399.80	3095.6	0.0010
$[\text{Mo}_{10.1}]^+[\text{tcb}]^-$	4.1062	8.300	386.29	2470.7	0.0063
$[\text{Im}_{10.1}]^+[\text{ntf}_2]^-$	3.8631	10.557	347.66	2632.0	0.0078
$[\text{Mo}_{10.1}]^+[\text{ntf}_2]^-$	3.5588	13.458	300.83	1216.3	0.1000
1-butanol	3.6139	2.751	259.59	2544.56	0.0067

^a2B association model for each IL and 1-butanol.

$$\text{ARD} = 100 \cdot \frac{1}{\text{NP}} \cdot \sum_{k=1}^{\text{NP}} \left| \left(1 - \frac{z_k^{\text{mod}}}{z_k^{\text{exp}}} \right) \right| \quad (19)$$

where NP is the number of data points.

Calculations for a variety of thermodynamic properties were performed and are discussed below. All the calculations and predictions were performed without introducing any binary interaction parameters.

The modeled densities of the pure ILs are in excellent accordance with the experimental data. This is illustrated in Figures 1 and 2. The resulting overall ARD of the liquid densities of the pure ILs at temperatures from 293.15 to 343.15 K is only 0.45%.

PC-SAFT was also applied to predict mixture densities for 1-butanol + IL solutions over the entire concentration range as well as for different temperatures. The predictions for the mixture densities are presented in Figures 3 and 4. PC-SAFT is able to accurately predict the concentration-dependent liquid densities for different temperatures with an ARD of 1.06%.

In addition to these calculations, PC-SAFT was capable of describing the partial pressures of 1-butanol in binary 1-butanol + IL solutions precisely. The modeling results for the concentration-dependent partial pressures of 1-butanol are illustrated in Figures 5 and 6. The overall ARD between the PC-SAFT modeling and the VPO data is 1.23%, while that between the PC-SAFT results and the HS-GC data is 2.30%. Slightly higher deviations are obtained for the HS-GC data as compared to the VPO data. This result may have been due to two reasons: (1) the HS-GC data is not used in the parameter estimation, and (2) there is a higher experimental uncertainty in the HS-GC data than in the VPO data. Investigations in this work have shown that including the activity coefficients at infinite dilution in the parameter-estimation procedure considerably improves PC-SAFT modeling of the concentrated IL solutions and produces accurate VLE calculations.

The experimental activity coefficients at infinite dilution determined in this study are in excellent accordance with the PC-SAFT calculations with an overall ARD of 1.22%. Figure 7 shows the modeling results for the 1-butanol activity coefficients at infinite dilution for the ILs considered over the temperature range investigated. It has to be noted again that all the pure-component PC-SAFT parameters are temperature-independent and binary interaction parameters have not been used.

The experimental VPO, HS-GC, and GLC data were combined to yield activity coefficients over the entire concentration range for comparison with the PC-SAFT modeling results. These results are illustrated in Figures 9 and 10. PC-SAFT is able to precisely model all four 1-butanol + IL solutions over the entire concentration range. The experimental HS-GC data that was not used in the parameter

estimation is also accurately modeled. The overall ARD is 0.82% for the VPO data and 2.15% for the HS-GC data.

In general, modeling the ILs containing the $[\text{ntf}_2]^-$ anion yields better results (lower deviations from experimental data) compared to ILs containing the $[\text{tcb}]^-$ anion. This may be explained by the more pronounced dissociation behavior of $[\text{tcb}]^-$ ILs compared to $[\text{ntf}_2]^-$ -based ILs, which is important especially at low IL concentrations.

CONCLUSION

New experimental data for the liquid densities of pure ILs, (1-butanol)–IL solution densities, and 1-butanol activity coefficients in 1-butanol + IL solutions were presented in this study. The following ILs were studied: 1-decyl-3-methyl-imidazolium tetracyanoborate ($[\text{Im}_{10.1}]^+[\text{tcb}]^-$), 4-decyl-4-methyl-morpholinium tetracyanoborate ($[\text{Mo}_{10.1}]^+[\text{tcb}]^-$), 1-decyl-3-methyl-imidazolium bis(trifluoromethylsulfonyl)imide ($[\text{Im}_{10.1}]^+[\text{ntf}_2]^-$), and 4-decyl-4-methyl-morpholinium bis(trifluoromethylsulfonyl)imide ($[\text{Mo}_{10.1}]^+[\text{ntf}_2]^-$). Measurements were made using the experimental techniques VPO, HS-GC, and GLC. The 1-butanol activity-coefficient data in the IL solutions was determined over the entire concentration range at 323.15 K by combining the data from the different experimental methods.

The (1-butanol)–IL interactions were characterized at the molecular level as a function of the IL concentration and the IL anion and cation types by analyzing the experimental data. The results showed that the partial pressures of 1-butanol in solutions with identical IL anions are very similar. ILs with the $[\text{Im}_{10.1}]^+$ cation cause only slightly lower partial pressures of 1-butanol compared to ILs with the $[\text{Mo}_{10.1}]^+$ cation. Thus, the $[\text{Im}_{10.1}]^+$ -based ILs show only slightly higher (1-butanol)–IL interactions compared to ILs with the $[\text{Mo}_{10.1}]^+$ cation. This behavior can be ascribed to the similar chemical structure of the cations considered. In contrast, the influence of the anions is considerably higher. ILs with $[\text{tcb}]^-$ anions cause lower partial pressures for 1-butanol than ILs with $[\text{ntf}_2]^-$. This behavior is ion-specific, as it was observed regardless of the type of cation and the IL concentration. The following trend summarizes the effect of the cations and anions on the (1-butanol)–IL interactions: $[\text{Im}_{10.1}]^+[\text{tcb}]^- > [\text{Mo}_{10.1}]^+[\text{tcb}]^- > [\text{Im}_{10.1}]^+[\text{ntf}_2]^- > [\text{Mo}_{10.1}]^+[\text{ntf}_2]^-$. Thus, the highest (1-butanol)–IL interactions of the ILs considered here were found for $[\text{Im}_{10.1}]^+[\text{tcb}]^-$.

Analyzing the data in terms of the association behavior of the ILs in 1-butanol, all the 1-butanol activity coefficients are observed to be higher than unity; that is, the IL ions strongly tend to form ion associates. In particular, the $[\text{ntf}_2]^-$ -based ILs strongly associate in 1-butanol, whereas the $[\text{tcb}]^-$ -based ILs are partially dissociated at low IL concentrations. This is also shown by analyzing the IL activity coefficients. In the solutions studied, all the IL activity coefficients are found to be below unity, and the series of their quantitative values is found to be in accordance with the results described above; that is, the ILs tend to form ion pairs in the sequence $[\text{Im}_{10.1}]^+[\text{tcb}]^- < [\text{Mo}_{10.1}]^+[\text{tcb}]^- < [\text{Im}_{10.1}]^+[\text{ntf}_2]^- < [\text{Mo}_{10.1}]^+[\text{ntf}_2]^-$.

PC-SAFT was used to model the experimental data. The pure-component parameters for the ILs were determined by fitting to pure-IL densities over a broad temperature range, to VPO data at 323.15 K, and to 1-butanol activity coefficients at infinite dilution at temperatures between 323.15 and 363.15 K. Binary interaction parameters were not required.

Using these parameter sets, PC-SAFT was able to accurately describe the thermo-physical properties and phase equilibria studied. Moreover, the solution densities of 1-butanol + IL could be quantitatively predicted over the entire concentration range for a broad temperature range. Thus, this model shows great promise for performing calculations and making predictions for other solvent + IL systems and in application to process-simulation tools.

AUTHOR INFORMATION

Corresponding Author

*E-mail: gabriele.sadowski@bci.tu-dortmund.de. Phone: +49 (231) 7552635.

Notes

The authors declare no competing financial interest.

ACKNOWLEDGMENTS

The authors gratefully acknowledge financial support from the Ministry of Innovation, Science and Research of North Rhine-Westphalia in the frame of CLIB-Graduate Cluster Industrial Biotechnology, Contract No. 314 - 108 001 08. The authors are also grateful to Merck KGaA for providing the ionic liquids and to Susanne Richter for her experimental work.

LIST OF SYMBOLS

Latin Characters

a (J/mol)	molar Helmholtz energy
a_i (-)	activity of component i
A_i (-)	headspace gas chromatography peak area of component i
B_{11} (cm^3/mol)	second virial coefficient of 1-butanol
B_{12} (cm^3/mol)	cross virial coefficient
\bar{h} (J/mol)	partial molar enthalpy
g (J/mol)	molar Gibbs energy
J (-)	correction factor
K (-)	osmometer calibration constant
k_B (J/K)	Boltzmann constant
k_{ij} (-)	binary interaction parameter for components i and j
M (g/mol)	molecular weight
m_i (mol/kg)	molality of component i (mol of component i / kg of solvent)
m_i^{seg} (-)	segment number of component i
NP (-)	number of data points
n (mol)	number of moles
p (Pa)	pressure
p^{out} (Pa)	column outlet pressure
p^{in} (Pa)	column inlet pressure
q (-)	number of parameters in power series
R (J/(mol K))	ideal gas constant
ΔR (mV)	resistance difference
\bar{s} (J/mol K)	partial molar entropy
T (K)	temperature
ΔT (K)	temperature difference
t_G (min)	retention time of the nonretainable component
t_R (min)	retention time
U_0 (m/s)	flow rate at column outlet
u_i/k_B (K)	dispersion-energy parameter of component i
V_N (m^3)	net retention volume
ν_1^∞ (m^3)	partial molar volume of 1-butanol in IL at infinite dilution

v_i (m ³ /mol)	liquid molar volume of component i
x_i (-)	mole fraction of component i
z_i (-)	quantity of component i
Z (-)	acentric factor

Greek Characters

α (-)	power series constants
γ_i (-)	activity coefficient of component i , related to the pure component state
γ_{IL}^* (-)	molality-based activity coefficient of IL, related to the infinite dilution
$\varepsilon^{A,B_i}/k_B$ (K)	association-energy parameter of component i
κ^{A,B_i} (-)	association-volume parameter of component i
ν (-)	stoichiometric coefficient
ρ (kg/m ³)	mass density
σ_i (Å)	segment diameter of component i
ϕ (-)	osmotic coefficient
φ_i (-)	fugacity coefficient of component i

Subscripts

0i	pure component
1	1-butanol
2	nitrogen
i	component i
ij	components i and j of a binary mixture
j	component j
k	sample number
r	index in power series
IL	ionic liquid

Superscripts

∞	infinite dilution
assoc	association
c	critical
disp	dispersion
E	excess
exp	experimental
hc	hard chain
L	liquid
mix	mixture
mod	modeled
polar	polar
r	index in power series
res	residual
V	vapor

Abbreviations

ARD	average relative deviation
GLC	gas-liquid chromatography
HS-GC	headspace-gas chromatography
IL	ionic liquid
[Im _{10.1}] ⁺	1-decyl-3-methyl-imidazolium
LiBr	lithium bromide
[Mo _{10.1}] ⁺	4-decyl-4-methyl-morpholinium
[ntf ₂] ⁻	bis(trifluoromethylsulfonyl)imide
PC-SAFT	perturbed-chain statistical associating fluid theory
[tcb] ⁻	tetracyanoborate
TCD	thermal conductivity detector
VLE	vapor-liquid equilibrium
VPO	vapor-pressure osmometry

REFERENCES

- (1) Brennecke, J. F.; Maginn, E. J. Ionic Liquids: Innovative Fluids for Chemical Processing. *AIChE J.* **2001**, *47* (11), 2384–2389.
- (2) Seddon, K. R. Ionic Liquids: A Taste of the Future. *Nat. Mater.* **2003**, *2* (6), 363–365.
- (3) Fredlake, C. P.; Crosthwaite, J. M.; Hert, D. G.; Aki, S. N. V. K.; Brennecke, J. F. Thermophysical Properties of Imidazolium-Based Ionic Liquids. *J. Chem. Eng. Data* **2004**, *49* (4), 954–964.
- (4) Roosen, C.; Mueller, P.; Greiner, L. Ionic Liquids in Biotechnology: Applications and Perspectives for Biotransformations. *Appl. Microbiol. Biotechnol.* **2008**, *81* (4), 607–614.
- (5) Oppermann, S.; Stein, F.; Kragl, U. Ionic Liquids for Two-phase Systems and Their Application for Purification, Extraction and Biocatalysis. *Appl. Microbiol. Biotechnol.* **2011**, *89* (3), 493–499.
- (6) Armand, M.; Endres, F.; MacFarlane, D. R.; Ohno, H.; Scrosati, B. Ionic-liquid Materials for the Electrochemical Challenges of the Future. *Nat. Mater.* **2009**, *8* (8), 621–629.
- (7) Plechkova, N. V.; Seddon, K. R. Applications of Ionic Liquids in the Chemical Industry. *Chem. Soc. Rev.* **2008**, *37* (1), 123–150.
- (8) Fadeev, A. G.; Meagher, M. M. Opportunities for Ionic Liquids in Recovery of Biofuels. *Chem. Commun.* **2001**, *3*, 295–296.
- (9) Han, X.; Armstrong, D. W. Ionic Liquids in Separations. *Acc. Chem. Res.* **2007**, *40* (11), 1079–1086.
- (10) Poole, C. F.; Poole, S. K. Extraction of Organic Compounds with Room Temperature Ionic Liquids. *J. Chromatogr., A* **2009**, *1217* (16), 2268–2286.
- (11) Heintz, A. Recent Developments in Thermodynamics and Thermophysics of Non-Aqueous Mixtures Containing Ionic Liquids. A Review. *J. Chem. Thermodyn.* **2005**, *37* (6), 525–535.
- (12) Calvar, N.; Gonzalez, B.; Dominguez, A.; Macedo, E. A. Osmotic Coefficients of Binary Mixtures of Four Ionic Liquids with Ethanol or Water at T = (313.15 and 333.15) K. *J. Chem. Thermodyn.* **2009**, *41* (1), 11–16.
- (13) Calvar, N.; Gonzalez, B.; Dominguez, A.; Macedo, E. A. Osmotic Coefficients of Binary Mixtures of 1-Butyl-3-methylimidazolium Methylsulfate and 1,3-Dimethylimidazolium Methylsulfate with Alcohols at T=323.15 K. *J. Chem. Thermodyn.* **2009**, *41* (5), 617–622.
- (14) Calvar, N.; Gomez, E.; Dominguez, A.; Macedo, E. A. Vapour Pressures, Osmotic and Activity Coefficients for Binary Mixtures Containing (1-Ethylpyridinium Ethylsulfate plus Several Alcohols) at T=323.15 K. *J. Chem. Thermodyn.* **2010**, *42*, 625–630.
- (15) Calvar, N.; Gonzalez, B.; Dominguez, A.; Macedo, E. A. Vapour Pressures and Osmotic Coefficients of Binary Mixtures of 1-Ethyl-3-methylimidazolium Ethylsulfate and 1-Ethyl-3-methylpyridinium Ethylsulfate with Alcohols at T=323.15 K. *J. Chem. Thermodyn.* **2009**, *41* (12), 1439–1445.
- (16) Calvar, N.; Gómez, E.; Domínguez, Á.; Macedo, E. A. Determination and Modelling of Osmotic Coefficients and Vapour Pressures of Binary Systems 1- and 2-Propanol with CnMimNTf₂ Ionic Liquids (n = 2, 3, and 4) at T = 323.15 K. *J. Chem. Thermodyn.* **2011**, *43* (8), 1256–1262.
- (17) Gomez, E.; Calvar, N.; Dominguez, A.; Macedo, E. A. Measurement and Modeling of Osmotic Coefficients of Binary Mixtures (Alcohol+1,3-Dimethylpyridinium Methylsulfate) at T=323.15 K. *J. Chem. Thermodyn.* **2011**, *43*, 908–913.
- (18) Shekaari, H.; Zafarani-Moattar, M. T. Osmotic Coefficients of some Imidazolium Based Ionic Liquids in Water and Acetonitrile at Temperature 318.15 K. *Fluid Phase Equilib.* **2007**, *254* (1–2), 198–203.
- (19) Shekaari, H.; Mousavi, S. S. Measurement and Modeling of Osmotic Coefficients of Aqueous Solution of Ionic Liquids Using Vapor Pressure Osmometry Method. *Fluid Phase Equilib.* **2009**, *279* (1), 73–79.
- (20) Shekaari, H.; Mousavi, S. S.; Mansoori, Y. Thermophysical Properties of Ionic Liquid, 1-Pentyl-3-methylimidazolium Chloride in Water at Different Temperatures. *Int. J. Thermophys.* **2009**, *30* (2), 499–514.
- (21) Shekaari, H.; Armanfar, E. Physical Properties of Aqueous Solutions of Ionic Liquid, 1-Propyl-3-methylimidazolium Methyl Sulfate, at T = (298.15 to 328.15) K. *J. Chem. Eng. Data* **2010**, *55* (2), 765–772.
- (22) Gardas, R. L.; Dagade, D. H.; Coutinho, J. A. P.; Patil, K. J. Thermodynamic Studies of Ionic Interactions in Aqueous Solutions of

- Imidazolium-based Ionic Liquids [Emim][Br] and [Bmim][Cl]. *J. Phys. Chem. B* **2008**, *112* (11), 3380–3389.
- (23) Sadr, M. H.; Sardroodi, J. J. Vapor Pressures and Osmotic Coefficients of the Acetone Solutions of Three Bis-(tetraalkylammonium)tetrathiomolybdates at 298.15 K Measured by Head-Space Gas chromatography. *Fluid Phase Equilib.* **2006**, *250* (1–2), 53–58.
- (24) Solie, T. N.; Hirs, C. H. W.; Timasheff, S. N. Vapor Pressure Osmometry. In *Methods in Enzymology*; Academic Press: New York, 1972; Vol. 26, pp 50–73.
- (25) Kim, H.-D.; Hwang, I.-C.; Park, S.-J. Isothermal Vapor–Liquid Equilibrium Data at $T = 333.15$ K and Excess Molar Volumes and Refractive Indices at $T = 298.15$ K for the Dimethyl Carbonate + Methanol and Isopropanol + Water with Ionic Liquids. *J. Chem. Eng. Data* **2010**, *55* (7), 2474–2481.
- (26) Heintz, A.; Kulikov, D. V.; Verevkin, S. P. Thermodynamic Properties of Mixtures Containing Ionic Liquids. 1. Activity coefficients at Infinite Dilution of Alkanes, Alkenes, and Alkylbenzenes in 4-Methyl-*n*-butylpyridinium Tetrafluoroborate Using Gas-Liquid Chromatography. *J. Chem. Eng. Data* **2001**, *46* (6), 1526–1529.
- (27) Heintz, A.; Kulikov, D. V.; Verevkin, S. P. Thermodynamic Properties of Mixtures Containing Ionic Liquids. 2. Activity Coefficients at Infinite Dilution of Hydrocarbons and Polar Solutes in 1-Methyl-3-ethyl-imidazolium Bis(trifluoromethyl-sulfonyl) Amide and in 1,2-Dimethyl-3-ethyl-imidazolium Bis(trifluoromethyl-sulfonyl) Amide Using Gas-Liquid Chromatography. *J. Chem. Eng. Data* **2002**, *47* (4), 894–899.
- (28) Shimizu, K.; Tariq, M.; Gomes, M. F. C.; Rebelo, L. P. N.; Lopes, J. N. C. Assessing the Dispersive and Electrostatic Components of the Cohesive Energy of Ionic Liquids Using Molecular Dynamics Simulations and Molar Refraction Data. *J. Phys. Chem. B* **2010**, *114* (17), 5831–5834.
- (29) Koddermann, T.; Wertz, C.; Heintz, A.; Ludwig, R. Ion-pair Formation in the Ionic Liquid 1-Ethyl-3-methylimidazolium Bis-(triflyl)imide as a Function of Temperature and Concentration. *ChemPhysChem* **2006**, *7* (9), 1944–1949.
- (30) Dorbritz, S.; Ruth, W.; Kragl, U. Investigation on Aggregate Formation of Ionic Liquids. *Adv. Synth. Catal.* **2005**, *347* (9), 1273–1279.
- (31) Vega, L. F.; Vilaseca, O.; Llovel, F.; Andreu, J. S. Modeling Ionic Liquids and the Solubility of Gases in Them: Recent Advances and Perspectives. *Fluid Phase Equilib.* **2010**, *294* (1–2), 15–30.
- (32) Paduszyński, K.; Domańska, U. Solubility of Aliphatic Hydrocarbons in Piperidinium Ionic Liquids: Measurements and Modeling in Terms of Perturbed-Chain Statistical Associating Fluid Theory and Nonrandom Hydrogen-Bonding Theory. *J. Phys. Chem. B* **2011**, *115* (43), 12537–12548.
- (33) Gross, J.; Sadowski, G. Perturbed-Chain SAFT: An Equation of State Based on a Perturbation Theory for Chain Molecules. *Ind. Eng. Chem. Res.* **2001**, *40* (4), 1244–1260.
- (34) Gross, J.; Sadowski, G. Application of the Perturbed-chain SAFT Equation of State to Associating Systems. *Ind. Eng. Chem. Res.* **2002**, *41* (22), 5510–5515.
- (35) Curras, M. R.; Vijande, J.; Pineiro, M. M.; Lugo, L.; Salgado, J.; Garcia, J. Behavior of the Environmentally Compatible Absorbent 1-Butyl-3-methylimidazolium Tetrafluoroborate with 2,2,2-Trifluoroethanol: Experimental Densities at High Pressures and Modeling of PVT and Phase Equilibria Behavior with PC-SAFT EoS. *Ind. Eng. Chem. Res.* **2011**, *50* (7), 4065–4076.
- (36) Ji, X.; Held, C.; Sadowski, G. Modeling Imidazolium-Based Ionic Liquids with ePC-SAFT. *Fluid Phase Equilib.* **2012**, *335* (0), 64–73.
- (37) Paduszyński, K.; Chiyen, J.; Ramjugernath, D.; Letcher, T. M.; Domańska, U. Liquid–Liquid Phase Equilibrium of (Piperidinium-based Ionic Liquid + an Alcohol) Binary Systems and Modelling with NRHB and PC-SAFT. *Fluid Phase Equilib.* **2011**, *305* (1), 43–52.
- (38) Wagner, W.; Pruss, A. The IAPWS Formulation 1995 for the Thermodynamic Properties of Ordinary Water Substance for General and Scientific Use. *J. Phys. Chem. Ref. Data* **2002**, *31* (2), 387–535.
- (39) Nasirzadeh, K.; Papaiconomou, N.; Neueder, R.; Kunz, W. Vapor Pressures, Osmotic and Activity coefficients of Electrolytes in Protic Solvents at Different Temperatures. 1. Lithium Bromide in Methanol. *J. Solution Chem.* **2004**, *33* (3), 227–245.
- (40) Everett, D. H. Effect of Gas Imperfection on Glc Measurements - A Refined Method for Determining Activity Coefficients and 2 Virial Coefficients. *Trans. Faraday Soc.* **1965**, *61*, 1637–1645.
- (41) Cruickshank, A. J. B.; Windsor, M. L.; Young, C. L. The Use of Gas-Liquid Chromatography to Determine Activity Coefficients and Second Virial Coefficients of Mixtures. I. Theory and Verification of Method of Data Analysis. *Proc. R. Soc. London, Ser. A* **1966**, *295*, 259–270.
- (42) Grant, D. W. *Gas-Liquid Chromatography*; Van Nostrand Reinhold Co: London, NY, 1971.
- (43) Tsonopoulos, C. Empirical Correlation of Second Virial Coefficients. *AIChE J.* **1974**, *20*, 263–272.
- (44) Poling, B. E.; Prausnitz, J. M.; O'Connell, J. P. *The Properties of Gases and Liquids*; McGraw-Hill: New York, 2001.
- (45) Kemme, H. R.; Kreps, S. I. Vapor Pressure of Primary *n*-Alkyl Chlorides and Alcohols. *J. Chem. Eng. Data* **1969**, *14* (1), 98–102.
- (46) Wolbach, J. P.; Sandler, S. I. Using Molecular Orbital Calculations to Describe the Phase Behavior of Cross-associating Mixtures. *Ind. Eng. Chem. Res.* **1998**, *37* (8), 2917–2928.
- (47) Held, C.; Neuhaus, T.; Sadowski, G. Compatible Solutes: Thermodynamic Properties and Biological Impact of Ectoines and Prolines. *Biophys. Chem.* **2010**, *152* (1–3), 28–39.
- (48) Domańska, U.; Marciniak, A. Physicochemical Properties and Activity Coefficients at Infinite Dilution for Organic Solutes and Water in the Ionic Liquid 1-Decyl-3-methylimidazolium Tetracyanoborate. *J. Phys. Chem. B* **2010**, *114* (49), 16542–16547.
- (49) Luckas, M.; Krissmann, J. *Thermodynamik der Elektrolytlösungen: Eine Einheitliche Darstellung der Berechnung Komplexer Gleichgewichte*; Springer: Berlin, 2001.
- (50) Heintz, A.; Verevkin, S. P.; Lehmann, J. K.; Vasiltsova, T. V.; Ondo, D. Activity Coefficients at Infinite Dilution and Enthalpies of Solution of Methanol, 1-Butanol, and 1-Hexanol in 1-Hexyl-3-methylimidazolium Bis(trifluoromethyl-sulfonyl) Imide. *J. Chem. Thermodyn.* **2007**, *39* (2), 268–274.
- (51) Reschke, T.; Naeem, S.; Sadowski, G. Osmotic Coefficients of Aqueous Weak Electrolyte Solutions: Influence of Dissociation on Data Reduction and Modeling. *J. Phys. Chem. B* **2012**, *116* (25), 7479–7491.
- (52) Nasirzadeh, K.; Neueder, R.; Kunz, W. Vapor Pressures, Osmotic and Activity Coefficients of Electrolytes in Protic Solvents at Different Temperatures. 3. Lithium Bromide in 2-Propanol. *J. Solution Chem.* **2005**, *34* (1), 9–24.
- (53) Tsiptsias, C.; Tsivintzelis, I.; Panayiotou, C. Equation-of-State Modeling of Mixtures with Ionic Liquids. *Phys. Chem. Chem. Phys.* **2010**, *12* (18), 4843–4851.